HOST-PATHOGEN INTERACTIONS

Parasitic Worms Stimulate Host NADPH Oxidases to Produce Reactive Oxygen Species That Limit Plant Cell Death and Promote Infection

Shahid Siddique,[1]* Christiane Matera,[1]* Zoran S. Radakovic,[1] M. Shamim Hasan,[1,2] Philipp Gutbrod,[1] Elzbieta Rozanska,[3] Miroslaw Sobczak,[3] Miguel Angel Torres,[4] Florian M. W. Grundler[1]†

Plants and animals produce reactive oxygen species (ROS) in response to infection. In plants, ROS not only activate defense responses and promote cell death to limit the spread of pathogens but also restrict the amount of cell death in response to pathogen recognition. Plants also use hormones, such as salicylic acid, to mediate immune responses to infection. However, there are long-lasting biotrophic plant-pathogen interactions, such as the interaction between parasitic nematodes and plant roots during which defense responses are suppressed and root cells are reorganized to specific nurse cell systems. In plants, ROS are primarily generated by plasma membrane–localized NADPH (reduced form of nicotinamide adenine dinucleotide phosphate) oxidases, and loss of NADPH oxidase activity compromises immune responses and cell death. We found that infection of *Arabidopsis thaliana* by the parasitic nematode *Heterodera schachtii* activated the NADPH oxidases RbohD and RbohF to produce ROS, which was necessary to restrict infected plant cell death and promote nurse cell formation. RbohD- and RbohF-deficient plants exhibited larger regions of cell death in response to nematode infection, and nurse cell formation was greatly reduced. Genetic disruption of *SID2*, which is required for salicylic acid accumulation and immune activation in nematode-infected plants, led to the increased size of nematodes in RbohD- and RbohF-deficient plants, but did not decrease plant cell death. Thus, by stimulating NADPH oxidase–generated ROS, parasitic nematodes fine-tune the pattern of plant cell death during the destructive root invasion and may antagonize salicylic acid–induced defense responses during biotrophic life stages.

INTRODUCTION

NADPH (reduced form of nicotinamide adenine dinucleotide phosphate) oxidase is a heteromultimeric enzyme complex involved in ROS production and immune response in a wide variety of organisms (*1*). The NADPH oxidase heavy chain subunit gp91^{phox} (also known as CYBB and NOX2) promotes the transfer of electrons to diatomic oxygen to generate superoxide anion (O_2^-) (*2*). The generation of superoxide starts a cascade of reactions that result in production of several highly reactive oxygen–derived small molecules collectively called reactive oxygen species (ROS).

Respiratory burst oxidase homologs (Rbohs), the plant homologs of *GP91PHOX*, are encoded by 10 genes in *Arabidopsis thaliana* (*RbohA* to *RbohJ*) (*3*–*5*). Rbohs generate ROS in response to bacterial and fungal pathogens (*3*, *6*), and genetic disruption of specific *Rbohs* alters plant responses to pathogens (*7*–*9*). In *A. thaliana*, loss of *RbohF* enhances cell death and increases resistance to a weakly virulent strain of the oomycete *Hyaloperonospora parasitica* (*3*). In contrast, in *Nicotiana benthamiana*, silencing of *RbohA* and *RbohB* reduces cell death and impairs plant resistance to infection by the oomycete *Phytophthora infestans* (*8*). These results point to a pathosystem-specific, sophisticated role of *Rbohs* in plant responses in infection.

Salicylic acid (SA) is a signaling molecule involved in plant defense against infection and interacts with ROS signaling. The concentration of SA increases in cells surrounding the infection site during the hypersensitive resistance response, a mechanism characterized by rapid death of the plant cells surrounding the infection site (*10*–*12*). ROS and SA form a feed-forward loop leading to induction of defense gene expression and cell death (*13*, *14*). In *A. thaliana*, loss of the gene encoding the zinc finger protein LSD1 (lesion stimulating disease 1), which inhibits SA-dependent cell death, results in runaway cell death phenotype (*15*). Plants with loss-of-function mutations in *LSD1* and *RbohD* or *LSD1* and *RbohF* have enhanced SA-induced cell death compared to those with *lsd1* mutations alone, suggesting that Rboh-derived ROS antagonize SA-dependent death signals to limit the spread of cell death during successful recognition of pathogens (*16*). Although there is evidence for a role of Rboh-derived ROS in resistance and cell death in different plant pathosystems, little is known about whether and how ROS might mediate biotrophic relationships.

Heterodera schachtii is a cyst nematode that establishes a biotrophic relationship with the roots of sugar beets and brassicaceaous plants, including *A. thaliana*. Second-stage juvenile (J2) nematodes invade plants primarily in the elongation zone above the root tips (*17*). After invasion, nematodes pierce individual root cells with their stylet, enter them, and travel through multiple cells to the vascular cylinder, leaving a path of collapsed, necrotic cells inside the root. In the vascular cylinder, nematodes use gentle stylet probing to identify cells that resist collapse and can serve as an initial syncytial cell (ISC) (*17*, *18*). Nematodes secrete factors through the stylet into the ISC that trigger partial dissolution of the cell wall and fusion of the ISC with neighboring root cells to form a multinucleate, hypertrophied, metabolically active nurse cell syncytium of more than 200 cells (*17*). Nematodes become sedentary and then form feeding tubes that connect the lumen of the stylet with the cytoplasm of the nurse cell. Feeding nematodes mature after three molts (J3, J4, and adult) over 2 weeks (*17*). Whereas females maintain interaction with the host plant, males cease

[1]Institute of Crop Science and Resource Conservation, Department of Molecular Phytomedicine, University of Bonn, 53115 Bonn, Germany. [2]Department of Plant Pathology, Faculty of Agriculture, Hajee Mohammad Danesh Science and Technology University, Dinajpur 5200, Bangladesh. [3]Department of Botany, Warsaw University of Life Sciences (SGGW), 02-787 Warsaw, Poland. [4]Centro de Biotecnología y Genomica de Plantas (UPM-INIA), ETSI Agrónomos, Universidad Politecnica de Madrid, Pozuelo de Alarcón, 28223 Madrid, Spain.
*These authors contributed equally to this work.
†Corresponding author. E-mail: grundler@uni-bonn.de

feeding after J3 (*19*). Accordingly, syncytia associated with female nematodes are larger than those associated with males (*20*). Moreover, under adverse conditions, such as nurse cell degeneration in resistant plant genotypes, more male than female nematodes develop. It is unknown whether this phenomenon results from epigenetic influences on sex determination or differences in the mortality of females and males (*21*, *22*). Here, we characterized the role of Rboh-dependent ROS in establishing a biotrophic relationship between *A. thaliana* and *H. schachtii*.

RESULTS

RbohD and RbohF promote nematode parasitism

RbohD or RbohF loss of function increases the susceptibility of host plants to infection by fungi or bacteria (*3*, *6*, *8*). We asked whether *A. thaliana* Rboh-family NADPH oxidases were involved in *H. schachtii* infection. We grew plants in agar medium under sterile conditions, and when the roots had spread through the agar, we inoculated cultures with 60 to 70 nematodes. We found that plants with loss-of-function mutations in *rbohD* or *rbohD* and *rbohF* (*rbohD/F*), but not *rbohA*, *rbohB*, *rbohC*, *rbohE*, *rbohF*, *rbohG*, or *rbohH*, showed reduced numbers of female nematodes present within roots 14 days after inoculation (dai) compared to wild-type (Col-0) plants (Fig. 1A and fig. S1A). In addition, the size of female nematodes and syncytia was significantly smaller in the *rbohD* or *rbohD/F* plants 14 dai (Fig. 1, B and C, and fig. S1, B and C). We also asked whether overexpression of *RbohD* in plants could affect nematode infection by assaying *35S::RbohD* transgenic plants (*16*), which expressed four times more *RbohD* in syncytium containing root segments than Col-0 plants (table S1). The total number of invaded nematodes and the average size of nematodes and syncytia were unchanged in *35S::RbohD* compared to Col-0 plants 14 dai (Fig. 1, A to C). Although the expansion of the syncytium reached its maximum size at about 14 dai, female nematodes continued to grow up to 4 weeks after inoculation. At 25 dai, we found that female nematodes were larger in *35S::RbohD* and smaller in *rbohD* or *rbohD/F* compared to Col-0 plants (Fig. 1D). Thus, RbohD is necessary but not sufficient to promote nematode invasion and growth and may be partially functionally redundant with RbohF in these processes.

To confirm the specificity of these observations, we used two complementary approaches. First, we used transgenic lines overexpressing *RbohD* in *rbohD* plants (*35S::RbohD/rbohD*). Unlike *rbohD* plants, *35S::RbohD/rbohD* plants did not show significant differences in the number of invaded nematodes or in the size of female nematodes or syncytia compared to Col-0 plants (fig. S2, A to D), suggesting that *35S::RbohD* complemented the *rbohD* mutation. Second, we treated plants with the compound diphenyliodonium (DPI), which inhibits Rboh activity (*23*, *24*). Col-0 plants treated with DPI had fewer invaded nematodes 14 dai compared to untreated control plants (Fig. 1E), and both female nematodes and syncytia were smaller (table S2).

DPI is an inhibitor of multiple flavoenzymes and could be toxic to nematodes. However, we found that rearing *Caenorhabditis elegans* larvae on nematode growth medium supplemented with DPI did not affect the number of eggs laid after 3 days (fig. S3A), suggesting that DPI does not affect nematode development and sexual maturation. Moreover, we found that incubating J2 *H. schachtii* in DPI for 5 days (approximately the time required for J2 nematodes to molt into J3 in plants) before inoculation decreased their ability to infect Col-0 plants (fig. S3B), but this effect was smaller than that seen when plants were treated with DPI (Fig. 1E). In addition, the size of female nematodes and syncytia was unchanged in DPI pretreated compared to control *H. schachtii* nematodes

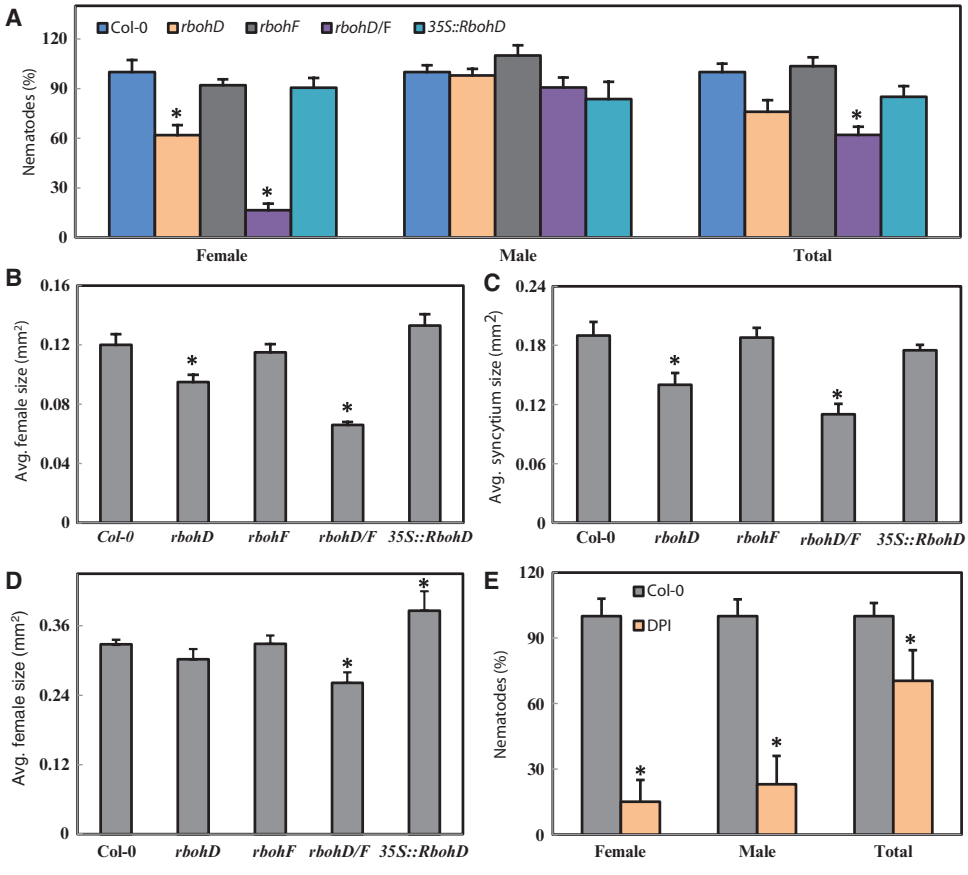

Fig. 1. Nematode infection assays in *Rboh* mutant, *RbohD* overexpressing, and DPI-treated plants. (**A**) Nematodes present in plant roots at 14 dai. Data points represent percent of nematodes where the number of nematodes per square centimeter of root area in Col-0 plants was set to 100%. (**B**) Average size of female nematodes 14 dai. (**C**) Average size of plant syncytia 14 dai. (**D**) Average size of female nematodes 25 dai. (**E**) Nematodes in DPI-treated plants 14 dai. Data points represent percent of nematodes where the number of nematodes per plant in Col-0 plants was set to 100%. For (A) to (E), data points represent three independent experiments (means ± SEM). Data were analyzed using single-factor analysis of variance (ANOVA) ($P < 0.05$). Asterisks indicate $P < 0.05$ compared to Col-0. Dunnett's tests were used for post hoc analyses.

(table S3). Thus, both genetic and pharmacological experiments suggest that Rboh activity is required in plants for successful nematode infection and growth.

Because *rbohD* and *rbohD/F* plants had reduced infection by nematodes, we characterized this process in more detail. We addressed whether reduced infection was due to decreased initial attraction of nematodes to roots by quantifying the number of successful invasions at an earlier time point. At 2 dai, there was no difference in nematode invasions between Col-0 and *rbohD* or *rbohD/F* plants (Fig. 2A). We also asked whether nematode migration or development within the plant was impeded by Rboh deficiency. Through repeated observations of the same invasion sites, we found that more nematodes left their initial invasion site in *rbohD/F* compared to Col-0 plants (Fig. 2B). In addition, more invaded nematodes were dead at 7 dai or failed to undergo sexual differentiation by 10 dai in *rbohD/F* compared to Col-0 plants (Fig. 2B). We assessed whether there could be defects in ISC establishment by monitoring for the cessation of stylet movements in nematodes that invaded roots 4 hours after inoculation (hai) and found that the average time to ISC establishment was increased in *rbohD/F* compared with Col-0 plants (Fig. 2C). Finally, we measured the growth of nematodes and syncytia after ISC establishment. We selected nematodes that successfully established an ISC at 2 dai to eliminate variability due to unsynchronized invasion and monitored their growth over 10 days. Both the nematodes (Fig. 2D) and syncytia (fig. S4) were significantly smaller by 3 dai and grew slower in *rbohD/F* compared to Col-0 plants. Thus, either RbohD or RbohF or both are required for nematode growth as well as ISC establishment and syncytium development, but not initial nematode invasion.

RbohD and RbohF are required for ROS production at early stages of nematode infection

Nematode infection triggers ROS production in plants (*25*). To identify whether RbohD and RbohF were required for this process in *H. schachtii*–infected roots, we visualized ROS with 3,3′-diaminobenzidine (DAB) (*26*) 1 dai. In the majority of Col-0 plants, DAB staining was increased at the site of nematode invasions (Fig. 3, A and B). However, the percent of invasion sites with increased DAB staining was reduced in *rbohD* or *rbohF* plants (Fig. 3, A, C, and D) and DPI-treated Col-0 plants (fig. S5) and eliminated in *rbohD/F* plants (Fig. 3, A and E). Overexpression of RbohD did not affect DAB staining in invaded roots (Fig. 3, A and F). Thus, RbohD and RbohF are required for ROS production during the initial stages of nematode infection.

To confirm the specificity of DAB-visualized ROS production, we labeled plants with 5-(and-6)-chloromethyl-2′,7′-dichlorodihydrofluorescein diacetate (CM-H_2DCFDA), which fluoresces when activated by ROS in living cells (*27*). We used confocal microscopy to monitor fluorescence in invaded roots of plants labeled with CM-H_2DCFDA 1 dai. We found that the extent of CM-H_2DCFDA fluorescence was increased in invaded roots of Col-0 (Fig. 3, G and H), but not *rbohD/F*, plants (Fig. 3I). Thus, during the early stages of nematode infection in plants, *RbohD* and *RbohF* produce ROS, which may support a biotrophic relationship.

RbohD and RbohF prevent cell death during syncytium formation

The delayed ISC selection by nematodes in *rbohD* and *rbohD/F* plants suggested that there could be anatomical changes in the roots that obstruct nematode migration. Using light and transmission electron microscopy, we examined cross sections of roots taken at the border of elongation and the root-hair zones associated with primary growth and at the lateral root formation zone associated with secondary thickening. The anatomy and growth of uninfected roots in both the primary (Fig. 4A) and secondary growth phases (fig. S6) were similar among Col-0 and *Rboh* mutant and overexpressing plants (*28*).

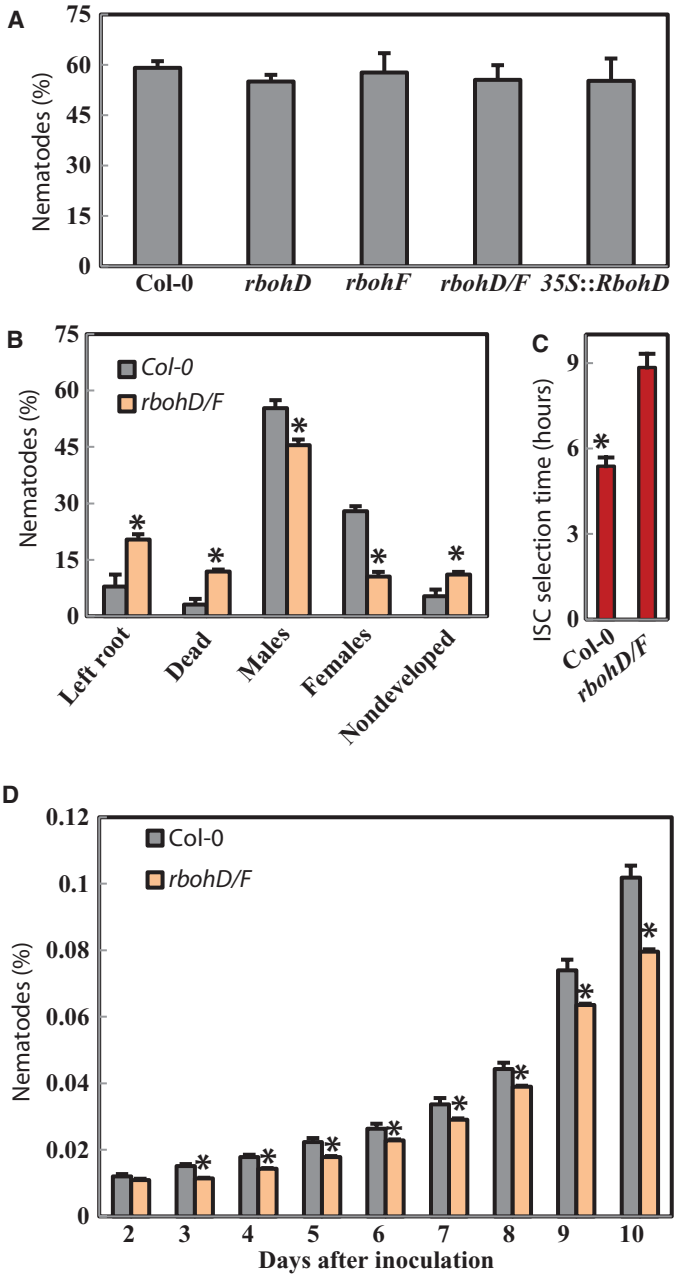

Fig. 2. Nematode infection assays in *Rboh* mutant plants. (A) Nematode invasion at 2 dai. Data represent percent of nematodes where the number of inoculated nematodes was set to 100%. (B) Observation of nematode behavior and development for 10 dai. Data represent percent of nematodes where the number of invaded nematodes was set to 100%. Left root, 3 dai. Dead, 7 dai. Nondeveloped, 10 dai. (C) ISC selection time. (D) Average size of female nematodes over 10 dai. For (A) to (C), data points represent three independent experiments (means ± SEM). Asterisks indicate $P < 0.05$ compared to Col-0 (*t* test).

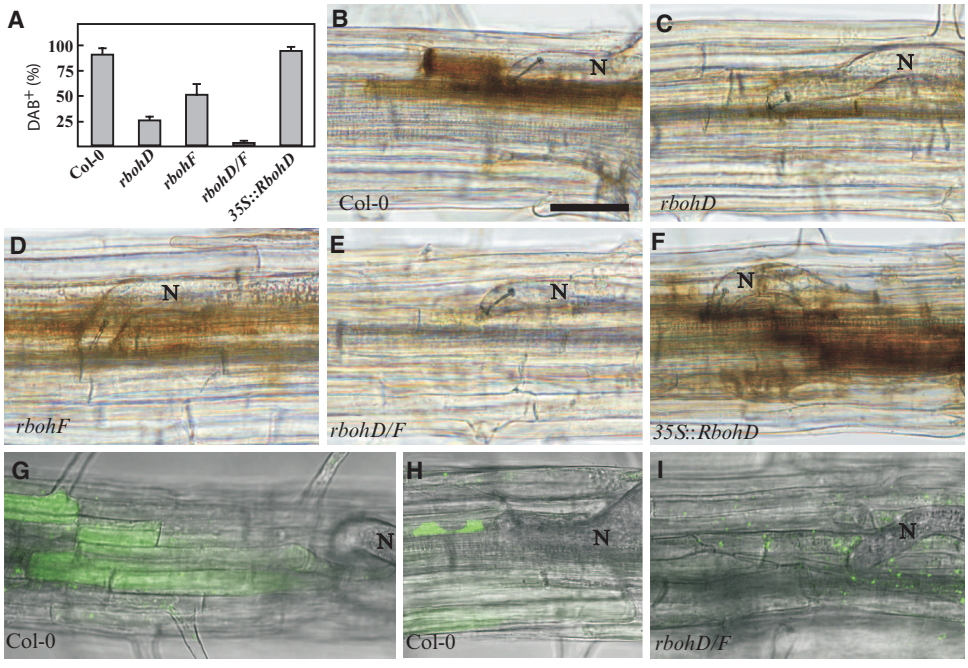

Fig. 3. Visualization of ROS in infected roots. (A) Quantification of DAB staining of ROS shown in (B) to (F). Data represent three independent experiments (means ± SEM). (B to F) DAB staining of ROS 1 dai on infected roots of plants with the indicated genotype. (G to I) CM-H_2DCFDA staining of ROS in living plant roots during migration (G and I) and ISC establishment (H). Scale bar, 50 μm. N, nematode.

To investigate structural changes in response to nematode infection, we analyzed cross sections of roots at 2, 5, and 14 dai. In Col-0, *rbohF*, and *35S::RbohD* plants, we found little evidence of necrosis (Fig. 4, A and B, and fig. S6). In contrast, in *rbohD* and *rbohD/F* plants, we found necrosis as early as 2 dai (Fig. 4A). Ultrastructural analysis suggested that these cells were outside the range of the nematode stylet and had osmiophilic deteriorated protoplasts and thickened cell walls (Fig. 4B). Moreover, depositions of callose-like material were present near cell walls neighboring necrotic cells (Fig. 4B). We found syncytia composed of several hypertrophied cells in Col-0, *rbohF*, and *35S::RbohD* plants 2 dai, whereas *rbohD* or *rbohD/F* plants contained no syncytia or only the ISC (Fig. 4, A and B). At 5 dai (Fig. 4, A and B, and fig. S7) and 14 dai (fig. S6), syncytia in *rbohF* or *35S::RbohD* roots resembled those in Col-0. In contrast, the few syncytia found in *rbohD* or *rbohD/F* roots at these times were smaller and composed of fewer and less hypertrophied cells (Fig. 4, A and B, and figs. S6 and S7). These syncytia had more osmiophilic cytoplasm with plastids containing starch grains (Fig. 4B and fig. S7), and the syncytial cell walls were thin with few openings (Fig. 4B and fig. S7). In *rbohD* or *rbohD/F* roots at 5 and 14 dai, some syncytia showed signs of cellular degradation such as an osmiophilic and flocculent or translucent cytoplasm (fig. S7), whereas other syncytia showed no features of degradation but were smaller in size and composed of fewer hypertrophied cells (fig. S7). These observations suggest that ISC selection is hampered in *rbohD* or *rbohD/F* plants and that necrosis of syncytia can occur at multiple times during its formation.

To confirm that *rbohD* or *rbohD/F* show enhanced syncytial necrosis, we quantified cell death using fluorescein diacetate (FDA) (*29*). We found a significant decrease in FDA fluorescence intensity in *rbohD/F* compared to Col-0 plants at 6 hai and 2 dai (Fig. 5), both during the early migratory stages and when nematodes are establishing the ISC, respectively. Col-0 plants treated with DPI also showed a significant decrease in FDA fluorescence compared to control-treated plants (fig. S8). Thus, cell death is enhanced in the absence of Rboh after nematode infection, implying that ROS produced by RbohD or RbohF or both during nematode migration and ISC selection prevents the activation of the plant defense responses, leading to cell death and enabling nematodes to establish syncytial nurse cells.

ROS limit cell death independent of SA

NADPH oxidases antagonize SA-dependent death-inducing signals during the hypersensitive resistance response in *A. thaliana* (*16*). We used real-time polymerase chain reaction (PCR) to assess changes in the expression of genes that are increased by SA or jasmonic acid signaling, or antioxidant accumulation. By analyzing root sections containing female nematode-associated syncytia 10 dai, we found that the expression of the SA-responsive genes *PR1*, *PR2*, and *PR5* increased in *rbohD/F* plants and that expression of *PR2* and *PR5* decreased in *35S::RbohD* compared to Col-0 plants (Fig. 6). Uninfected roots of *rbohD/F* and *35S::RbohD* plants did not show detectable changes in the expression of *PR* genes compared to control (fig. S9). In contrast, the expression of genes that respond to jasmonic acid signaling and antioxidant accumulation were not consistently changed in *rbohD/F* and *35S::RbohD* plants (Fig. 6 and fig. S9). Thus, the reduced growth of nematodes in *rbohD/F* plants could be due to the activation of local SA-mediated defense responses at infection sites.

To assess whether enhanced cell death in infected *rbohD/F* plants was due to failure in activation of SA-dependent cell death signals, we focused on SID2, a protein in the isochorismate synthase pathway (*30*). Plants with *SID2* loss of function have basal SA but do not increase SA in response to infection (*30*). Thus, we predicted that mutation of *SID2* could increase nematode infection as well as nematode and syncytia size in *rbohD/F* plants. We found that *sid2* plants had more invaded nematodes relative to Col-0 plants at 14 dai (Fig. 7A), indicating that SID2-dependent SA is required to limit nematode infection. However, the size of female nematodes (Fig. 7B) and syncytia (Fig. 7C) did not differ between *sid2* and Col-0 plants, suggesting that SID2 does not interfere with syncytium development or nematode growth. In *rbohD/F sid2* triple-mutant plants (*rbohD/F/sid2*), both the number of invaded nematodes (Fig. 7A) and the size of syncytia (Fig. 7C) were comparable to those of *rbohD/F* plants. Moreover, the size of female nematodes was comparable in *rbohD/F/sid2*, *sid2*, and Col-0 plants (Fig. 7B). Thus, the defect in nematode growth in *rbohD/F* plants is likely independent of SID2-dependent SA, and the retarded growth of female nematodes in *rbohD/F* plants could depend on SA-mediated defense responses.

We assessed whether SID2-dependent SA was required for enhanced cell death in *rbohD/F* plants responding to nematode infection. If SID2 was required for nematode resistance in *rbohD/F* plants, then we would expect to see that *rbohD/F/sid2* plants had reduced cell death compared to *rbohD/F* plants. *rbohD/F/sid2* plants had a significant decrease in

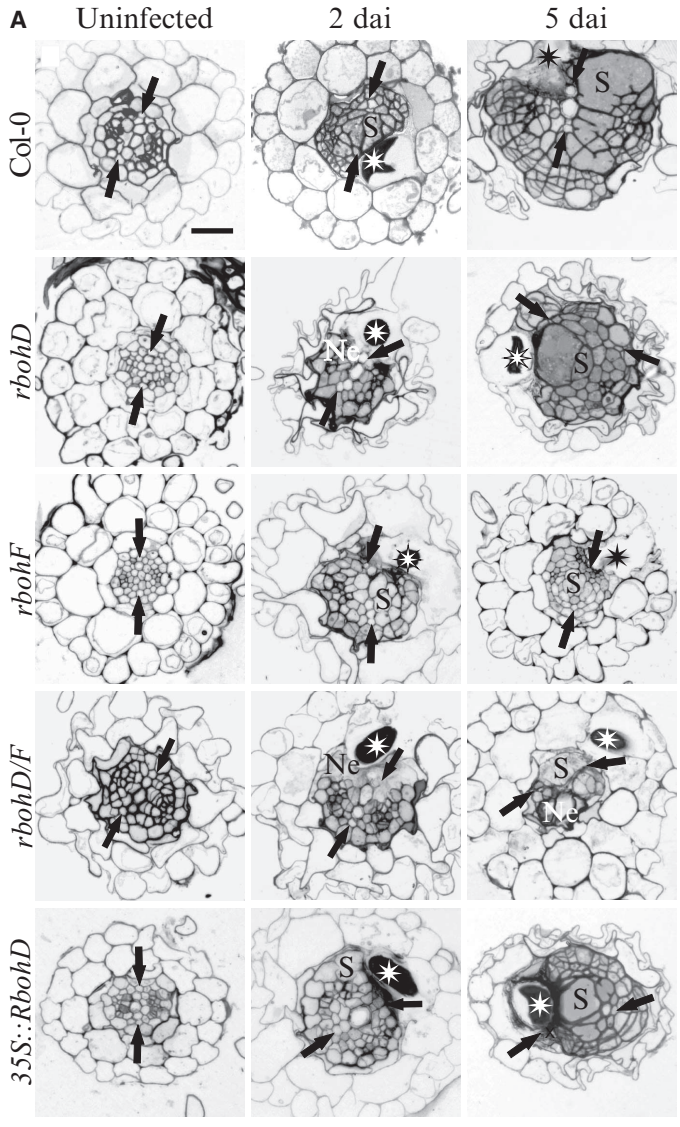

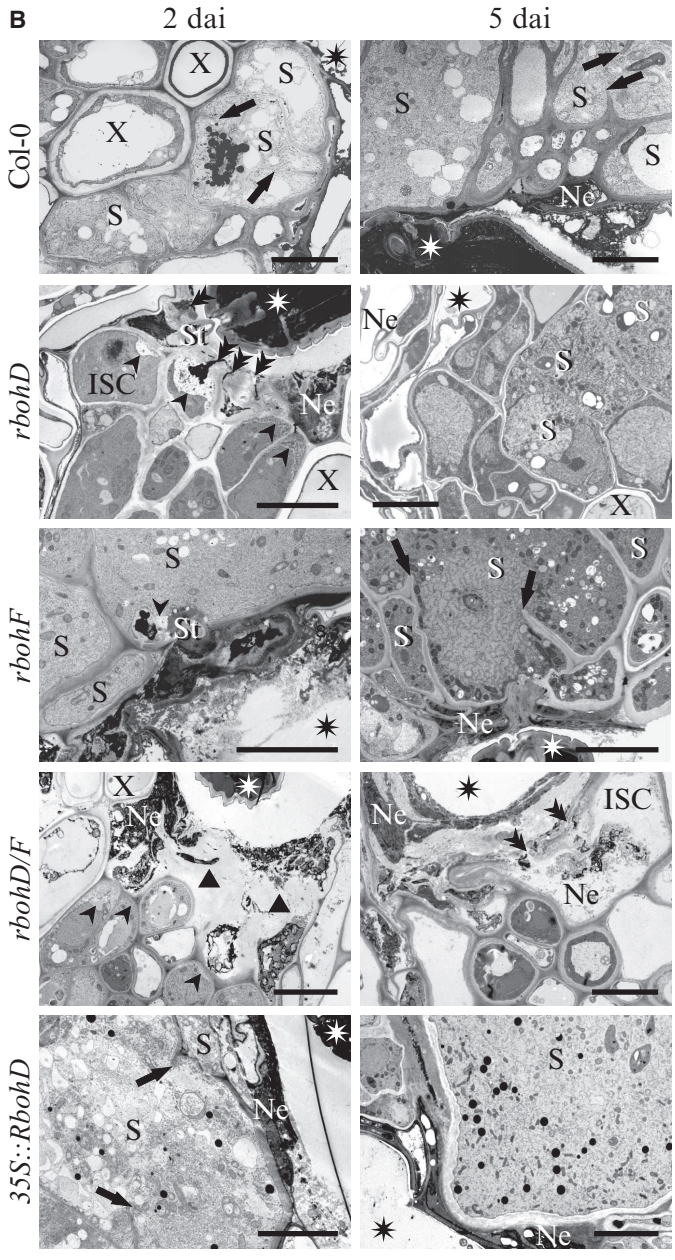

Fig. 4. Microscopic analysis of root anatomy and the development of nematode-induced syncytia in *Rboh* mutant and overexpressing plants. (**A**) Light microscopy micrographs of sections taken at root-hair zone of uninfected plants (left column) and at the nematode head region of infected roots 2 dai (middle column) or 5 dai (right column). Asterisks mark the nematode. Arrows indicate the position of primary xylem bundles. (**B**) Transmission electron microscopy micrographs of sections taken at nematode head region from 2 dai (left column) and 5 dai (right column) roots. Asterisks mark the nematode or the position of the nematode if the section was taken above its head or the head was located outside the field of view. Arrows point to cell wall stubs in syncytia. Triangles mark thickened cell walls. Arrowheads indicate callose depositions, and double arrowheads point to stylet insertion places. Ne, necrosis; S, syncytium; St, stylet; X, xylem vessel. Scale bars, 20 μm (A) and 5 μm (B).

the intensity of the FDA fluorescence at 6 hai compared to Col-0, but not *rbohD/F*, plants (Fig. 7D). These data support the model that the incompatibility of *rbohD/F* plants with the initial establishment of ISC is independent of *SID2*-dependent SA.

We found that loss of RbohD and RbohF increased the expression of SA-dependent genes in nematode-infected plants. To test whether SA was downstream of RbohD and RbohF, we assessed the expression of SA-dependent genes in *rbohD/F/sid2* plants. The expression of *PR1*, *PR2*, and *PR5* was at or below the limit of detection in infected root segments of *rbohD/F/sid2* plants, despite normal amounts of 18*S* (table S4). Thus, we were not able to calculate a fold difference relative to Col-0 plants. Nevertheless, there was no qualitative evidence of a large increase in expression of *PR1*, *PR2*, and *PR5* in *rbohD/F/sid2* compared to Col-0 plants, suggesting that SA-dependent gene expression is inhibited downstream of RbohD and RbohF during nematode infection.

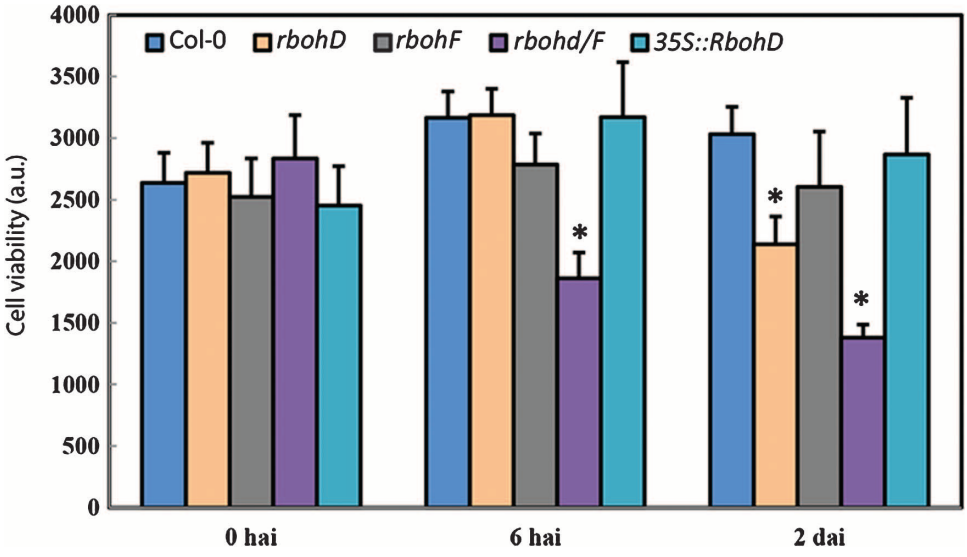

Fig. 5. Cell viability in infected or uninfected root sections of *Rboh* mutant and overexpressing plants. Cell viability depicted as the fluorescence intensity in arbitrary units (a.u.) of FDA staining in plants at the indicated times after inoculation. Data represent eight independent experiments with six root segments per genotype per experiment (means ± SEM). Data were analyzed using ANOVA ($P < 0.05$). Asterisks indicate $P < 0.05$ compared to Col-0. Dunnett's tests were used for post hoc analyses.

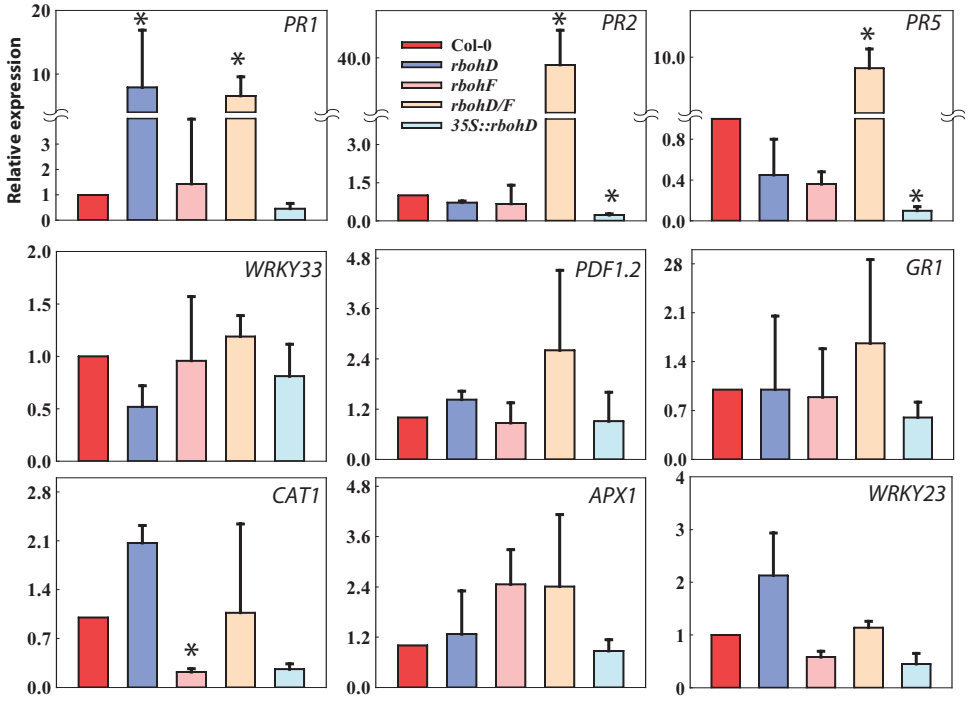

Fig. 6. Gene expression analysis on root segments with developing syncytia 10 dai. Data represent relative expression of the indicated genes with the value in Col-0 plants set to one. Data represent three independent experiments (mean + range). Asterisks indicate $P < 0.05$ compared to Col-0 (*t* test).

DISCUSSION

Rapid production of ROS (oxidative bursts) in the apoplast by NADPH oxidases is an early defense response after the successful recognition of pathogens by the plant immune system (*3*, *6*–*8*). Our analysis revealed that RbohD and RbohF are the main sources of host ROS produced during cyst nematode infections in *A. thaliana*. We predicted that host defense signals downstream of ROS would be inhibited by nematode-derived pathogenicity factors. However, we identified a previously uncharacterized function for RbohD- and RhobF-dependent ROS in facilitating nematode infection and feeding site development.

We propose that the infection of *A. thaliana* by *H. schachtii* proceeds in two phases: In the first phase, nematode invasion of roots and subsequent migration causes cellular damage that triggers cell death. NADPH oxidase–produced ROS disrupt the relay of death-inducing signals between the directly damaged and surrounding cells, thereby preventing the spread of cell death and supporting nematode infection. ROS also contribute to the process of ISC establishment. Thus, the increased cell death seen in *rbohD/F* plants (Figs. 4 and 5) could result from a failure of nematodes to establish syncytia. However, we found that cell death was increased in *rbohD/F* at the site of nematode invasion as early as 6 hai, when the nematodes were still in the migration phase (Fig. 5), suggesting that the failure of ISC establishment is not sufficient to explain all of the increased cell death in these plants. Moreover, because we found that mutation of *SID2* did not enhance nematode infection (Fig. 7A) or decrease early cell death in *rbohD/F* plants (Fig. 7D), we infer that this initial wave of increased cell death is independent of pathogen-induced SA signaling.

In the second phase of nematode infection, the establishment of the ISC and subsequent syncytium expansion is a prerequisite for biotrophic parasitism of the nematode. ROS signaling at infection site inactivates SA-mediated defense responses and enables the growth of nematodes. Consistent with this model, we found that female nematodes that were able to establish syncytia were significantly smaller in *rbohD/F* compared to Col-0 plants (Fig. 7B), but those in *rbohD/F/sid2* plants were not (Fig. 7B). It is possible that the decreased nematode size results indirectly from increased plant cell death in *rbohD/F* plants,

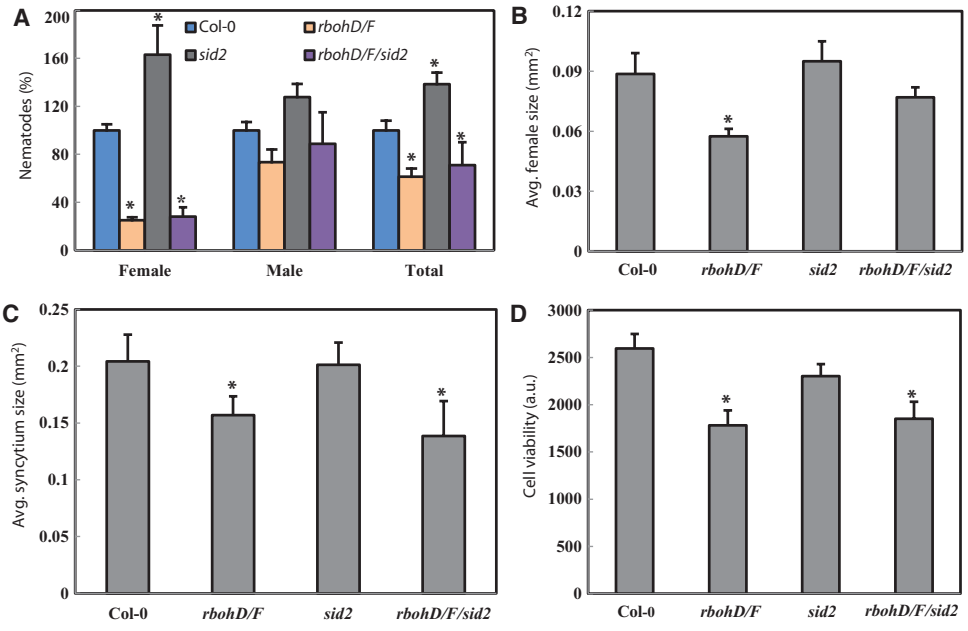

Fig. 7. Nematode infection assay and cell viability in *rbohD/F/sid2* plants. (A) Nematodes present in plant roots 14 dai. Data points represent percent of nematodes where the number of nematodes per plant in Col-0 was set to 100%. (B) Average size of female nematodes 14 dai. (C) Average size of plant syncytia 14 dai. (D) Cell viability depicted as the fluorescence intensity (in arbitrary units) of FDA staining in plants 6 hai. Data represent 10 independent experiments (means ± SEM). Data were analyzed using ANOVA ($P < 0.05$). Asterisks indicate $P < 0.05$ compared to Col-0. Dunnett's tests were used for post hoc analyses.

which would reduce the number of cells available to be included in the syncytia.

Our model is compatible in part with previous findings showing that pathogen-induced ROS suppress the spread of SA-mediated cell death signals in plants after infection (*16*, *31*). It was suggested that RbohD suppresses the spread of cell death by controlling the levels of antioxidants in cells at and around the infection site (*16*). In contrast, we found that the expression of antioxidant genes, *glutathione reductase 1*, *catalase 1*, and *ascorbate peroxidase 1*, did not change in *rbohD/F* roots with established syncytia. Thus, the role of Rbohs in the protection from SA-mediated cell death may not involve these genes.

This model raises the question of whether nematodes release factors that actively stimulate the formation of ROS. *H. schachtii* was found to secrete the effector protein 10A06 into host cells, which interacts with host spermidine synthase 2, leading to increased polyamine oxidase activity in syncytia (*32*). Increased polyamine oxidase may increase the production of ROS that serve as signaling molecules at low concentration for the development or function of syncytia (*32*).

Syncytium formation in host roots is accompanied by widespread transcriptional and metabolic changes in both the infected and systemic plant tissues (*33*, *34*), and ROS could alter these changes. We found that RbohD and RbohF have the capacity to influence SA-dependent gene expression in infected roots. However, Rboh activity may play a broader role in syncytium development and function. Moreover, the fact that RbohD mediates systemic signaling in response to diverse stimuli (*23*) suggests that ROS could be involved in systemic signaling between nurse cells and the host plant.

Suppression of death-inducing signals by ROS in compatible biotrophic interactions is previously uncharacterized. Our results provide further understanding of the molecular mechanism that enables pathogens with destructive invasive behavior to switch to a biotrophic life-style, leading to the establishment of a long-term feeding relationship with the host plant, suggesting a process in the coevolution of a nematode and host plant during which the parasite gains the ability to use NADPH oxidase–mediated cell death regulation to its own benefit.

MATERIALS AND METHODS

Plant material and growth conditions

A. thaliana plants were grown in petri dishes containing agar medium supplemented with modified Knop's nutrient solutions under conditions described previously (*35*). The *rboh* mutants and *35S::RbohD* strains have been described (*3*, *16*). The *Sid2* mutant strain was the allele *sid2-2/eds16-1* (*30*). *rbohD/F/sid2* plants were generated by crossing and confirmed by PCR. The primers are listed in table S5.

Nematode infection assays

Nematodes were inoculated onto the surface of agar medium in petri dishes. For each experiment, 30 plants were used for each genotype. The number of male and female nematodes per plant was counted at 14 dai. Alternatively, the number of nematodes per square centimeter of root area was calculated for *rbohdD*, *rbohF*, *rbohD/F*, or *35S::RbohD* plants for the data shown in Fig. 1A to rule out the influence of root area on nematode infection. For the root area calculation, the plants were photographed with a DM2000 dissection microscope (Leica Microsystems) at the time of infection, and the area was calculated using Leica Application Suite (LAS) software (Leica Microsystems). The average size of syncytia and associated nematodes was measured in longitudinal optical sections as described previously (*21*). Briefly, 50 infection sites in roots containing syncytia and nematodes were photographed with a Leica DM2000 dissection microscope at 14 dai. The syncytia or females were outlined, and the area was calculated using LAS software (Leica Microsystems).

DPI experiments

For experiments with DPI, Col-0 plants were grown as described above. After 5 days, seedlings were transferred to petri dishes containing agar medium supplemented with DPI (1 μM) and used for nematode infection assays. In experiments designed to test the direct effect of DPI on *H. schachtii* invasion, freshly hatched J2 nematodes were incubated with DPI (1 μM) for 5 days at room temperature. Then, the nematodes were collected and resuspended in 0.7% (w/v) GelRite (Duchefa) containing DPI (1 μM) to ensure prolonged contact with DPI. For the *C. elegans* development experiments, nematodes were reared in nematode growth medium (*36*) supplemented with DPI at the indicated concentrations. Synchronized L1 larvae were obtained by sodium hypochloride treatment (*36*). Nematodes were fed *Escherichia coli* OP50. Egg lays were counted after 3 days from three replicates.

Nematode behavioral assays

For nematode invasion assays (Fig. 2A), the number of nematodes invading the roots at 2 dai was counted. To assess nematode migration, death, and sexual development (Fig. 2B), nematodes invading the roots 1 or 2 dai were selected (with permanent marker on the petri dishes), and their behavior was followed during the next 10 days by taking photographs every 24 hours. For each experiment, 20 nematodes were examined for each plant genotype. For ISC selection experiments (Fig. 2C), nematodes that were invading the root at 4 hai were marked with permanent marker on the petri dishes, and their stylet movements were observed hourly for 16 hours. ISC selection was defined as the time when a nematode stopped stylet movements. For each experiment, 20 to 30 nematodes were observed for each plant genotype. For the long-term growth experiments (Fig. 2D), nematodes that established ISC at 1 dai were marked with permanent marker on the petri dishes and imaged daily. For each experiment, 30 to 40 nematodes were examined for each plant genotype.

ROS detection

To visualize H_2O_2, a type of ROS, roots were stained with DAB using a modification of the protocol described in (*28*). At 1 dai, infected roots were incubated in DAB solution (1 mg/ml in water) at room temperature for 3 to 5 hours in a high-humidity box. The samples were then fixed in a solution of ethanol/lactic acid/glycerol (3:1:1). Root segments without lateral root primordia, mechanical stress, and root tips were selected for imaging with a Leica DM4000 microscope (Leica Microsystems) equipped with an Olympus C-5050 digital camera. The average number of stained spots was calculated for 50 nematodes per plant genotype. For CM-H_2DCFDA (C6827, Molecular Probes) staining, plants were grown on coverslips. At 1 dai, the agar was carefully removed from around root segments containing nematodes. Root segments were incubated with CM-H_2DCFDA (10 μM) in phosphate-buffered saline for 90 min at 4°C (*3*). After incubation, the samples were washed with KCl (0.1 mM) and $CaCl_2$ (0.1 mM) to remove excess CM-H_2DCFDA. The samples were kept at room temperature for 1 hour and then imaged with a Zeiss CLSM 710.

Cell viability labeling

Root segments were cut (0.5 cm) and transferred to half-strength Murashige and Skoog basal medium (MS medium, Sigma-Aldrich) containing FDA (5 μg/ml) (*29*). FDA stocks (2 mg/ml in acetone) were stored at −20°C. Root segments without lateral roots or root tips were used for staining. After 10 min of incubation, root segments were washed five times with MS medium without FDA. The fluorescence emission intensities were measured at 535 nm after excitation at 485 nm by using a microplate reader (Infinite 200 Pro, Tecan) (*29*). For each experiment, six root segments were used per plant genotype.

Microscopic analysis

Root segments were dissected, fixed, dehydrated, and embedded in epoxy resin as described previously (*21*). Light and transmission electron microscopy analyses were conducted on sections obtained from the same samples. Root segments were serially sectioned on an RM2165 microtome (Leica Microsystems) into 2-μm sections. Sections were collected on glass slides, stained with an aqueous solution of crystal violet dye (1%, Sigma-Aldrich), and imaged on an AX70 Provis (Olympus) light microscope equipped with an Olympus DP50 digital camera (Olympus). At selected places, ultrathin sections (90 nm) were taken for transmission electron microscopy with a UCT ultramicrotome (Leica). Ultrathin sections were stained with a saturated ethanol solution of uranyl acetate (Sigma-Aldrich) followed by lead citrate (Sigma-Aldrich) and imaged on an FEI 268D Morgagni transmission electron microscope (FEI Company) equipped with an SIS Morada digital camera (Olympus SIS). Digital images were adjusted for similar contrast and brightness, cropped, and resized using Adobe Photoshop software.

Real-time PCR

Root segments (up to 200) containing syncytia associated with female nematodes were dissected at 10 dai. Total RNA was extracted using a NucleoSpin RNA kit (Macherey-Nagel) according to the manufacturer's instructions, including deoxyribonuclease digestion. Reverse transcription was performed with the High-Capacity cDNA Reverse Transcription Kit (Invitrogen) according to the manufacturer's instructions. Quantitative PCR was performed with the Stepone Plus Real-Time PCR System (Applied Biosystems). Each sample contained 10 μl of Fast SYBR Green qPCR Master Mix with uracil-DNA, glycosylase, and 6-carboxy-x-rhodamine (Invitrogen), 2 mM $MgCl_2$, 0.5 μl each of forward and reverse primers (10 μM), 2 μl of complementary DNA (cDNA), and water in a 20-μl total reaction volume. The primers are listed in table S5. Samples were analyzed in three technical replicates. 18*S* was used as an internal control. Relative expression was calculated by the $\Delta\Delta C_t$ method (*37*), where the expression of each gene was normalized to 18*S* and then to Col-0 to calculate fold change. The range shown in Fig. 6 was calculated from three experimental replicates (*37*).

SUPPLEMENTARY MATERIALS

www.sciencesignaling.org/cgi/content/full/7/320/ra33/DC1

Fig. S1. Nematode infection assays in *Rboh* mutant plants.
Fig. S2. Nematode infection assays in *35S::RbohD/rbohD* plants.
Fig. S3. Development and invasion of nematodes treated with DPI.
Fig. S4. Plant syncytium size in *rbohD/F* plants.
Fig. S5. ROS visualization in roots of DPI-treated Col-0 plants.
Fig. S6. Light microscopy of uninfected *Rboh* mutant plants in secondary growth and infected *Rboh* mutant plants 14 dai.
Fig. S7. Transmission electron microscopy of *Rboh* mutant plants 5 and 14 dai.
Fig. S8. Cell viability in nematode-infected and uninfected plants treated with DPI.
Fig. S9. Analysis of gene expression in uninfected roots.
Table S1. Expression of *RbohD* and *RbohF* in syncytia of *35S::RbohD* plants.
Table S2. Nematode and syncytium size in DPI-treated Col-0 plants 14 dai.
Table S3. Nematode and syncytium size in Col-0 plants 14 dai with nematodes preincubated with DPI.
Table S4. Expression of PR genes in Col-0 and *rbohD/F/sid2* uninfected roots.
Table S5. Primers sequences used in this study.

REFERENCES AND NOTES

1. B. H. Segal, M. J. Grimm, A. N. H. Khan, W. Han, T. S. Blackwell, Regulation of innate immunity by NADPH oxidase. *Free Radic. Biol. Med.* **53**, 72–80 (2012).
2. J. D. Lambeth, NOX enzymes and the biology of reactive oxygen. *Nat. Rev. Immunol.* **4**, 181–189 (2004).
3. M. A. Torres, J. L. Dangl, J. D. G. Jones, *Arabidopsis* gp91^{phox} homologues *AtrbohD* and *AtrbohF* are required for accumulation of reactive oxygen intermediates in the plant defense response. *Proc. Natl. Acad. Sci. U.S.A.* **99**, 517–522 (2002).
4. Q. J. Groom, M. A. Torres, A. P. Fordham-Skelton, K. E. Hammond-Kosack, N. J. Robinson, J. D. G. Jones, *rbohA*, a rice homologue of the mammalian *gp91phox* respiratory burst oxidase gene. *Plant J.* **10**, 515–522 (1996).
5. M. A. Torres, H. Onouchi, S. Hamada, C. Machida, K. E. Hammond-Kosack, J. D. G. Jones, Six *Arabidopsis thaliana* homologues of the human respiratory burst oxidase (*gp91^{phox}*). *Plant J.* **14**, 365–370 (1998).
6. N. Doke, Involvement of superoxide anion generation in the hypersensitive response of potato-tuber tissues to infection with an incompatible race of *Phytophthora infestans* and to the hyphal wall components. *Physiol. Plant Pathol.* **23**, 345–357 (1983).
7. C. Lamb, R. A. Dixon, The oxidative burst in plant disease resistance. *Annu. Rev. Plant Physiol. Plant Mol. Biol.* **48**, 251–275 (1997).
8. H. Yoshioka, N. Numata, K. Nakajima, S. Katou, K. Kawakita, O. Rowland, J. D. G. Jones, N. Doke, *Nicotiana benthamiana* gp91^{phox} homologs *NbrbohA* and *NbrbohB* participate in H_2O_2 accumulation and resistance to *Phytophthora infestans*. *Plant Cell* **15**, 706–718 (2003).

9. D. Marino, C. Dunand, A. Puppo, N. Pauly, A burst of plant NADPH oxidases. *Trends Plant Sci.* **17**, 9–15 (2012).
10. W. E. Durrant, X. Dong, Systemic acquired resistance. *Annu. Rev. Phytopathol.* **42**, 185–209 (2004).
11. D. A. Dempsey, J. Shah, D. F. Klessig, Salicylic acid and disease resistance in plants. *Crit. Rev. Plant Sci.* **18**, 547–575 (1999).
12. J. Durner, J. Shah, D. F. Klessig, Salicylic acid and disease resistance in plants. *Trends Plant Sci.* **2**, 266–274 (1997).
13. J. Draper, Salicylate, superoxide synthesis and cell suicide in plant defence. *Trends Plant Sci.* **2**, 162–165 (1997).
14. K. Overmyer, M. Brosché, J. Kangasjärvi, Reactive oxygen species and hormonal control of cell death. *Trends Plant Sci.* **8**, 335–342 (2003).
15. R. A. Dietrich, M. H. Richberg, R. Schmidt, C. Dean, J. L. Dangl, A novel zinc finger protein is encoded by the Arabidopsis *LSD1* gene and functions as a negative regulator of plant cell death. *Cell* **88**, 685–694 (1997).
16. M. A. Torres, J. D. G. Jones, J. L. Dangl, Pathogen-induced, NADPH oxidase–derived reactive oxygen intermediates suppress spread of cell death in *Arabidopsis thaliana*. *Nat. Genet.* **37**, 1130–1134 (2005).
17. U. Wyss, F. M. W. Grundler, Feeding behavior of sedentary plant parasitic nematodes. *Netherlands J. Plant Pathol.* **98**, 165–173 (1992).
18. M. Sobczak, W. A. Golinowski, F. M. W. Grundler, Ultrastructure of feeding plugs and feeding tubes formed by *Heterodera schachtii*. *Nematology* **1**, 363–374 (1999).
19. M. Sobczak, W. Golinowski, F. M. W. Grundler, Changes in the structure of *Arabidopsis thaliana* roots induced during development of males of the plant parasitic nematode *Heterodera schachtii*. *Eur. J. Plant Pathol.* **103**, 113–124 (1997).
20. J. Muller, K. Rehbock, U. Wyss, Growth of *Heterodera schachtii* with remarks on amounts of food consumed. *Revue Nematol.* **4**, 227–234 (1981).
21. S. Siddique, S. Endres, J. M. Atkins, D. Szakasits, K. Wieczorek, J. Hofmann, C. Blaukopf, P. E. Urwin, R. Tenhaken, F. M. W. Grundler, D. P. Kreil, H. Bohlmann, Myo-inositol oxygenase genes are involved in the development of syncytia induced by *Heterodera schachtii* in Arabidopsis roots. *New Phytol.* **184**, 457–472 (2009).
22. D. L. Trudgill, Effect of environment on sex determination in *Heterodera rostochiensis*. *Nematologica* **13**, 263–272 (1967).
23. G. Miller, K. Schlauch, R. Tam, D. Cortes, M. A. Torres, V. Shulaev, J. L. Dangl, R. Mittler, The plant NADPH oxidase RBOHD mediates rapid systemic signaling in response to diverse stimuli. *Sci. Signal.* **2**, ra45 (2009).
24. C. K. Auh, T. M. Murphy, Plasma membrane redox enzyme is involved in the synthesis of O_2^- and H_2O_2 by *Phytophthora* elicitor-stimulated rose cells. *Plant Physiol.* **107**, 1241–1247 (1995).
25. G. H. Waetzig, M. Sobczak, F. M. W. Grundler, Localization of hydrogen peroxide during the defence response of *Arabidopsis thaliana* against the plant-parasitic nematode *Heterodera glycines*. *Nematology* **1**, 681–686 (1999).
26. H. Thordal-Christensen, Z. G. Zhang, Y. D. Wei, D. B. Collinge, Subcellular localization of H_2O_2 in plants. H_2O_2 accumulation in papillae and hypersensitive response during the barley–powdery mildew interaction. *Plant J.* **11**, 1187–1194 (1997).
27. K. A. Kristiansen, P. E. Jensen, I. M. Møller, A. Schulz, Monitoring reactive oxygen species formation and localisation in living cells by use of the fluorescent probe CM-H_2DCFDA and confocal laser microscopy. *Physiol. Plant* **136**, 369–383 (2009).
28. L. Dolan, K. Janmaat, V. Willemsen, P. Linstead, S. Poethig, K. Roberts, B. Scheres, Cellular organisation of the *Arabidopsis thaliana* root. *Development* **119**, 71–84 (1993).
29. X. Y. Qiang, B. Zechmann, M. U. Reitz, K. H. Kogel, P. Schäfer, The mutualistic fungus *Piriformospora indica* colonizes *Arabidopsis* roots by inducing an endoplasmic reticulum stress–triggered caspase-dependent cell death. *Plant Cell* **24**, 794–809 (2012).
30. M. C. Wildermuth, J. Dewdney, G. Wu, F. M. Ausubel, Isochorismate synthase is required to synthesize salicylic acid for plant defence. *Nature* **414**, 562–565 (2001).
31. M. Pogány, U. von Rad, S. Grün, A. Dongó, A. Pintye, P. Simoneau, G. Bahnweg, L. Kiss, B. Barna, J. Durner, Dual roles of reactive oxygen species and NADPH oxidase RBOHD in an Arabidopsis-*Alternaria* pathosystem. *Plant Physiol.* **151**, 1459–1475 (2009).
32. T. Hewezi, P. J. Howe, T. R. Maier, R. S. Hussey, M. G. Mitchum, E. L. Davis, T. J. Baum, Arabidopsis spermidine synthase is targeted by an effector protein of the cyst nematode *Heterodera schachtii*. *Plant Physiol.* **152**, 968–984 (2010).
33. D. Szakasits, P. Heinen, K. Wieczorek, J. Hofmann, F. Wagner, D. P. Kreil, P. Sykacek, F. M. W. Grundler, H. Bohlmann, The transcriptome of syncytia induced by the cyst nematode *Heterodera schachtii* in Arabidopsis roots. *Plant J.* **57**, 771–784 (2009).
34. J. Hofmann, A. El Ashry, S. Anwar, A. Erban, J. Kopka, F. Grundler, Metabolic profiling reveals local and systemic responses of host plants to nematode parasitism. *Plant J.* **62**, 1058–1071 (2010).
35. P. C. Sijmons, F. M. W. Grundler, N. von Mende, P. R. Burrows, U. Wyss, *Arabidopsis thaliana* as a new model host for plant-parasitic nematodes. *Plant J.* **1**, 245–254 (1991).
36. T. Stiernagle, Maintenance of *C. elegans*, in *C. elegans: A Practical Approach*, I. Hope, Ed. (Oxford University Press, Oxford, 2006).
37. K. J. Livak, T. D. Schmittgen, Analysis of relative gene expression data using real-time quantitative PCR and the $2^{-\Delta\Delta CT}$ method. *Methods* **25**, 402–408 (2001).

Acknowledgments: We acknowledge the technical support of G. Sichtermann, U. Schlee, S. Neumann, T. Gerhardt, J. Holbein, and B. Klinzer. We are thankful to D. Szakasits for her critical revision of the manuscript. We appreciate the valuable comments of J. Dangl on the manuscript. We acknowledge M. Hoch for giving us access to the confocal microscope and the microplate reader. **Funding:** M.A.T. was supported by grant (2007)D/562971 from the International Reintegration Program from the European Union. E.R. and M.S. were supported by grant 116/N-COST/2008/0 from The Polish Ministry of Science and Higher Education. **Author contributions:** S.S. and F.M.W.G. designed the research and wrote the paper. S.S. and C.M. conducted the majority of experiments. M.S.H. and P.G. conducted gene expression experiments. Z.S.R. carried out infection assays with triple mutants. E.R. and M.S. carried out the microscopic analyses. M.A.T. identified mutant combinations. All authors commented on the manuscript. **Competing interests:** The authors declare that they have no competing financial interests. **Data and materials availability:** Materials used in this study are available on request.

Submitted 1 October 2013
Accepted 21 March 2014
Final Publication 8 April 2014
10.1126/scisignal.2004777
Citation: S. Siddique, C. Matera, Z. S. Radakovic, M. S. Hasan, P. Gutbrod, E. Rozanska, M. Sobczak, M. A. Torres, F. M. W. Grundler, Parasitic worms stimulate host NADPH oxidases to produce reactive oxygen species that limit plant cell death and promote infection. *Sci. Signal.* **7**, ra33 (2014).

Parasitic Worms Stimulate Host NADPH Oxidases to Produce Reactive Oxygen Species That Limit Plant Cell Death and Promote Infection

Shahid Siddique, Christiane Matera, Zoran S. Radakovic, M. Shamim Hasan, Philipp Gutbrod, Elzbieta Rozanska, Miroslaw Sobczak, Miguel Angel Torres and Florian M. W. Grundler

Sci. Signal. **7** (320), ra33.
DOI: 10.1126/scisignal.2004777originally published online April 3, 2014

Promoting Parasitism with ROS

Some species of nematode worms can invade the roots of plants and establish a feeding site composed of a large syncytial plant cell. This biotrophic lifestyle requires that the worms find a way to suppress plants' immune responses. One aspect of plant immunity is the production of reactive oxygen species (ROS) that damage pathogens and promote plant cell death to limit the spread of infection. Siddique *et al.* found that deleting the enzymes that produce ROS in *Arabidopsis thaliana* plants responding to infection by *Heterodera schachtii* worms prevented the worms from establishing syncytia and growing within roots, suggesting that the worms have co-opted plant ROS as a means of promoting parasitism. Thus, plant ROS can play both positive and negative roles during infection.

Science Signaling (ISSN 1937-9145) is published by the American Association for the Advancement of Science, 1200 New York Avenue NW, Washington, DC 20005.